Morphology, Properties and Application of Iron Oxide/Polycaprolactone Nanocomposites

[1,2]Khalid Saeed, [1]Noshi Khan, [1]Tariq Shah and [1]Muhammad Sadiq
[1]*Department of Chemistry, University of Malakand, Chakdara, Dir (L), Khyber Pakhtunkhwa, Pakistan.*
[2]*Department of Chemistry, Bacha Khan University Charsadda, Khyber Pakhtunkhwa, Pakistan.*
khalidkhalil2002@yahoo.com*

(Received on 29th April 2020, accepted in revised form 24th August 2020)

Summary: Polycaprolactone (PCL) and Fe_2O_3/PCL nanocomposites sheets/films were prepared by solution casting method. The morphological study illustrated that Fe_2O_3 nanoparticles were dispersed and embedded well within the PCL matrix. The size of Fe_2O_3 nanoparticles were below 250 nm. The thermal stability of Fe_2O_3/PCL nanocomposites was lower than neat PCL, which might be due to Fe_2O_3 (act as catalyst during the thermal degradation of PCL). The differential scanning calorimetry (DSC) analyses show that the crystallization temperature of the nanocomposites was slightly enhanced as compared to neat PCL. The polarized optical microscopy (POM) analyses showed that the size of Fe_2O_3/PCL nanocomposites spherulites were smaller than neat PCL. The photodegradation study presented that the nanocomposites photodegraded higher quantity of rhodamine B dye as compared to neat PCL. The neat PCL degraded about 24 and 72% while Fe_2O_3 (6 wt%)/PCL nanocomposites degraded about 72 and 98% of dye within 2 and 10 h, respectively.

Keywords: Polycaprolactone, Nanocomposites, Spherulites, Photodegradation, Iron oxide nanoparticles.

Introduction

The nanocomposites are multi phases where one of the phases has one, two or three dimensions of less than 100 nm. In metal/polymer nanocomposites, the metal has dimensions of tens of nanometers or less. The nanoparticles exhibit distinctive physicochemical properties like large surface area, mechanically strong, optically active and chemically reactive, which make the nanoparticles exceptional and suitable applicants for various applications like electronic, magnetic, optical, and mechanical properties.

In polymer based nanocomposites, the polymers are used as matrix phase, and nanofillers like nanoparticles, nanotubes, nanofibers, nanoplatelets and nanowires, are added as filler or reinforcement to the matrix. Polymers are widely used in industries because of the ease of production and their ductile and lightweight nature. However, it has poor thermal, electrical and mechanical properties than metals and ceramics, which can be overcome by using various types of nanofillers. Traditionally, these nanocomposites have been obtained by mechanical mixing of metal nanoparticles and dissolved or melted polymers and as a result a homogeneous dispersion of metal nanoparticles occurs in highly viscous matrices. The preparation of metal filled polymer composites (nano heterogeneous composite materials) are of interest in the areas of actuators, catalysis, sensors, optical, and electronic devices etc. [1,2].

In Recent years, arising of carcinogenic and mutagenic compounds in environment have been generally observed. Such hazardous compounds have long degradation time in the environment and are toxic or non biodegradable to microorganisms. Environmental contaminations are due to the wastewaters produced from the textile industries and dyestuff industrial processes [3]. Photocatalytic treatment is the best way to reduce the contamination of water. In order to decrease harm caused by organic dyes pollution to environment and human, different photocatalysts were used to degrade organic compounds in water to convert them into harmless chemicals. For example; Nanoclay supported copper oxide nanoparticles, heterostructure photocatalysts, manganese dioxide NPs/activated carbon composite and Ag_3PO_4/graphene-oxide composite was used for the photodegradation of methyl orange dye [4-7]. Usually, the process of photodegradation involved band to band excitation of semiconductor particles by light to create •OH radicals resulting from valence band hole oxidation of terminal OH^- groups and water of hydration on particle surface. These reactive radicals are oxidizing agent which appear to control overall kinetics of oxidation process [8-11]. In this manner metal oxide nanoparticles such as ZnO/SnO_2 and WO_3/TiO_2, Cu/TiO_2 composites are the types of semiconductors which were successfully synthesized. Composites materials are not only used for catalytic activities but also for various applications such as gas sensors, electric conductivity and so on [12]. Recently Panda et al. [13] deliberates the catalytic

*To whom all correspondence should be addressed.

activity of Fe_2O_3-SiO_2 composite which has successfully decolorized methyl orange dye. Beside the inorganic composites materials, it was also reported that the incorporation of inorganic materials into polymers and porous materials exhibit reasonable catalytic activities under light illumination [14].

PCL is well known for its unique properties like degradability, biocompatibility and use in medical supplies as drug delivery system and degradable packing [15]. But the main disadvantage is its low melting point, which may affect its applications. The blending of PCL with other polymers or nanofillers is the most suitable technique to overcome this disadvantage. While the selection of Fe_3O_3 nanoparticles is due low cost, easily availability and are mostly used for the degradation of aromatic organic compounds in industrial waste water [16].

In present study, PCL and Fe_2O_3/PCL nanocomposites films or sheets were prepared by solution casting technique. The neat PCL and Fe_2O_3/PCL nanocomposites films were not only characterized by various instrumental techniques such as SEM, TGA, DSC and POM but also used as photocatalysts for the decolorization of rhodamine B dye in aqueous medium.

Experimental

Materials

Iron chloride and chloroform was purchased from Sigma Aldrich. The polycaprolactone were prepared in our laboratory (average molecular weight 90,000).

Synthesis of Iron Oxide nanoparticles

The 100 mL Iron chloride solution (0.1 M) were taken in 250 mL flask and then 20 mL NaOH (1 M) was added drop wise into the flask until pH reached up to 8-9. The reaction mixture was heated at 60 ^oC for 1h with continuous stirring. After the specific reaction time, the mixture was cooled and the prepared Fe_2O_3 nanoparticles were separated via filtration. The Fe_2O_3 nanoparticles were washed several times with deionized water to remove unreacted chemicals. The Fe_2O_3 nanoparticles were then dried in an oven at 100 ^oC and stored.

Preparation of pure PCL and Fe_2O_3/PCL polymer nanocomposite

PCL film/sheets were prepared by solution casting method by the same method as discussed somewhere else [17]. 3g PCL was dissolved in 10 mL chloroform and stirred it for 30 min. The polymer films were then prepared by casting the viscous solution of PCL, which is spread on a clean glass surface. The blend film/sheet was obtained after evaporation of chloroform from the viscous solution of PCL. The films were dried, labeled and stored for analysis. The same practice was adopted for the preparation of F_2O_3 (1, 2, 4 and 6 wt%)/PCL nanocomposites.

Photodegradation of Rhodamine B

Neat PCL and F_2O_3/PCL nanocomposites samples and 10 mL Rhodamine B (15 ppm) solution were taken separately in different vials and then placed beneath UV light (254 nm, 15 W) for specific time (2, 4, 6, 8, 10 h). After the specific irradiation time, the neat PCL and F_2O_3/PCL nanocomposites of different percent were separated. The dye degradation study was carried out by UV-VIS absorption spectrophotometer. The %degradation of rhodamine B was calculated as:

$$\text{Degradation rate } (\%) = \left(\frac{Co - C}{Co}\right) \times 100$$

$$\text{Degradation rate } (\%) = \left(\frac{Ao - A}{Ao}\right) \times 100$$

where Co and C is the concentration of dye, before and after UV irradaition, Ao shows initial absorbance, and A is the dye absorbance after UV irradaition.

Instrumentation

The morphological study of gold-coated PCL and Fe_2O_3/PCL nanocomposites was performed by JEOL, JSM-5910 SEM. The TGA curves of the PCL and Fe_2O_3/PCL nanocomposites were attained in an inert atmosphere with heating rate of 20 ^oC/min between 25 ^oC and 700 ^oC, using a Diamond TG/DTA Perkin Elmer. The DSC characterization was carried out by Perkin Elmer Diamond Series DSC, USA. The POM images of PCL and Fe_2O_3/PCL were obtained by a BX-51 POM. The sample was melted on a heater and squeezed between 2 glass slides for 10 min. The photodegradation study of rhodamine B was performed by UV–VIS spectrophotometer (UV-1800, Shimadzu, Japan).

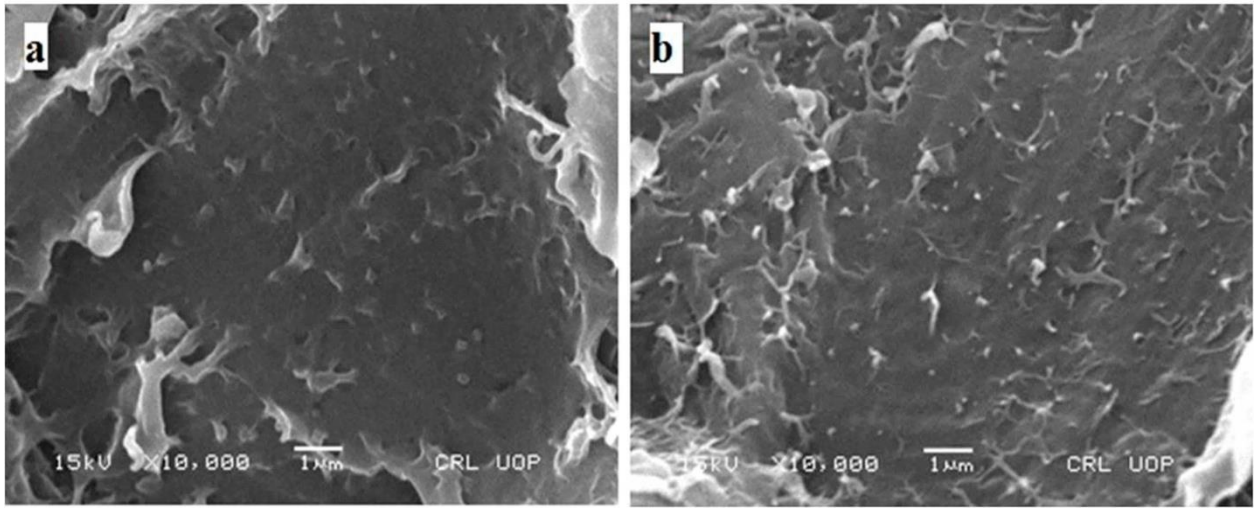

Fig. 1: SEM micrographs of (a) Fe_2O_3 (4 wt%)/PCL and (b) Fe_2O_3 (6 wt%)/PCL nanocomposites.

Results and discussion

Morphology of Fe_2O_3/PCL Nanocomposites

The SEM micrographs (Fig 1 a,b) presented that both 4 and 6 wt% Fe_2O_3 nanoparticles are present in dispersed form within the polymer matrix. The sizes of the nanoparticles were below 250 nm. The dispersion of Fe_2O_3 nanoparticles within the matrix indicated that Fe_2O_3 nanoparticles were compatible with PCL polymer matrix. The excellent dispersion of Fe_2O_3 nanoparticles inside PCL matrix enables larger number of active catalytic centers for the photocatalytic reaction.

Thermal study of Pure PCL and Fe_2O_3/PCL Nanocomposites

The TG thermograms of pure PCL and (2, 4 and 6 wt%) Fe_2O_3/PCL nanocomposites are shown in Fig 2. The TG curves showed that the weight of all samples remained constant initially. The neat PCL begin weight lose at 335 ^oC and completely decompose at 446 ^oC while in the case of nanocomposites samples the degradation temperature declined gradually as increased the amount of the nanoparticles. While the 2, 4 and 6 wt% Fe_2O_3/PCL nanocomposites started weight loss at about 320, 300 and 292 ^oC, respectively. The thermograms also presented that the major portion of nanocomposite were degraded at about 425 ^oC. The decrease in the degradation temperature might be due the Fe_2O_3 nanoparticles, which act as catalyst and as results the degradation temperature of the PCL was decreased by the addition of nanoparticles. The residual quantities in nanocomposites, which contribute to the Fe_2O_3 nanoparticles were remained at high temperature.

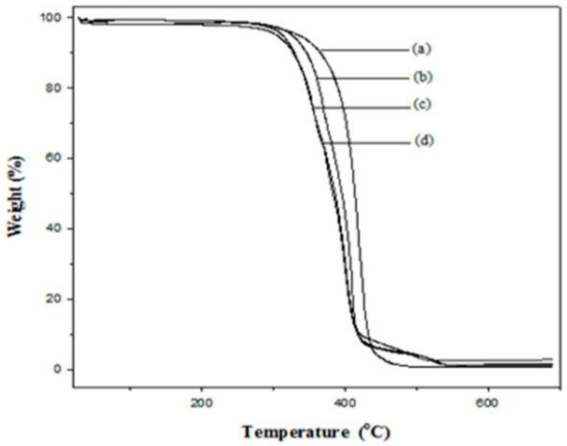

Fig. 2: TG curves of (a) pure PCL, (b) Fe_2O_3(2 wt%)/PCL, (c) Fe_2O_3(4 wt%)/PCL and (d) Fe_2O_3(6 wt%)/PCL.

DSC is one of the most suitable techniques in evaluation of first order transition like melting and crystallization. Pure PCL and Fe_2O_3/PCL nanocomposites were subjected to DSC analyses in order to study the effect of Fe_2O_3 nanoparticles on the melting and crystallization temperature of PCL. Fig. 3 presented the DSC thermograms of crystallization temperature (Tc) of neat PCL and Fe_2O_3/PCL nanocomposites. The neat PCL shows Tc at about 33.5 ^oC while the Tc curves of Fe_2O_3/PCL nanocomposites were shifted towards slightly higher temperature (about 34.4 ^oC). The increase in Tc of PCL by the addition of Fe_2O_3 nanoparticles might be due to the nucleation of Fe_2O_3 nanoparticles [18].

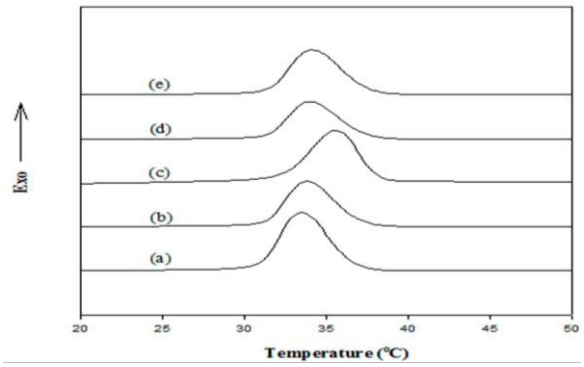

Fig. 3: DSC Tc thermograms of (a) pure PCL, (b) Fe_2O_3 (1 wt%) /PCL nanocomposites, (c) Fe_2O_3 (2 wt%) /PCL, (d) Fe_2O_3 (4 wt%) /PCL and (e) Fe_2O_3 (6 wt%) /PCL.

Fig 4 illustrated the DSC thermograms of melting temperature (Tm) of PCL and Fe_2O_3/PCL nanocomposites. The Tm of neat PCL was about 57.4 ^oC whereas the Tm of Fe_2O_3/PCL were decreased gradually upto 56.6 ^oC as increased in the amount of nanoparticles in to polymer matrix. The decline in Tm in the case of Fe_2O_3/PCL nanocomposites might be due to the nanoscale interaction between the Fe_2O_3 nanoparticles surface and the polymer and as result less stable crystal were formed during crystallization from the melt state [19].

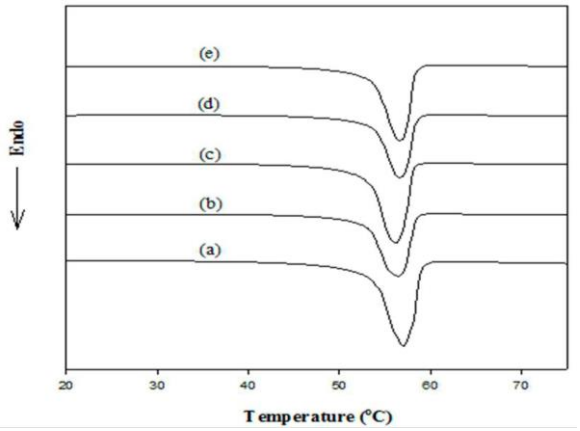

Fig. 4: DSC Tm thermograms of (a) pure PCL, (b) Fe_2O_3 (1 wt%) /PCL nanocomposites, (c) Fe_2O_3 (2 wt%) /PCL, (d) Fe_2O_3 (4 wt%) /PCL and (e) Fe_2O_3 (6 wt%) /PCL.

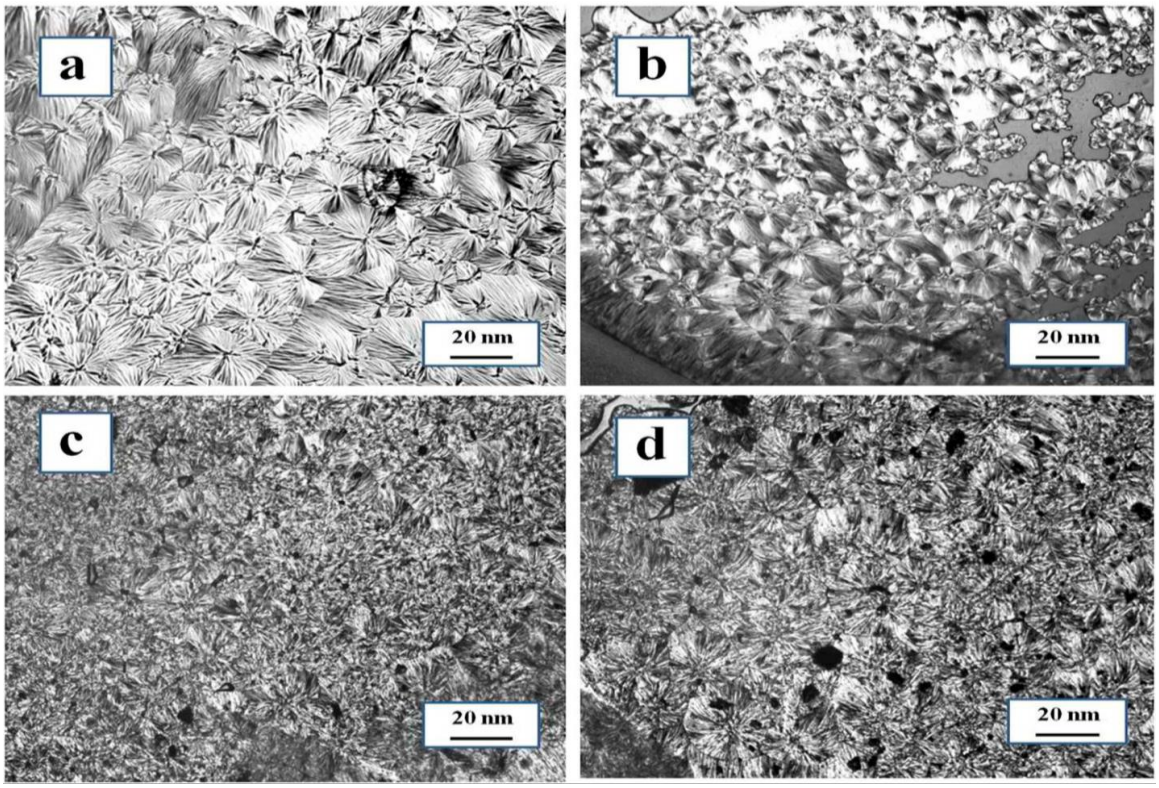

Fig. 5: POM micrographs of (a) PCL, b) Fe_2O_3 (1 wt%) /PCL nanocomposites, (c) Fe_2O_3 (2 wt%) /PCL, (d) Fe_2O_3 (4 wt%) /PCL and (e) Fe_2O_3 (6 wt%) /PCL.

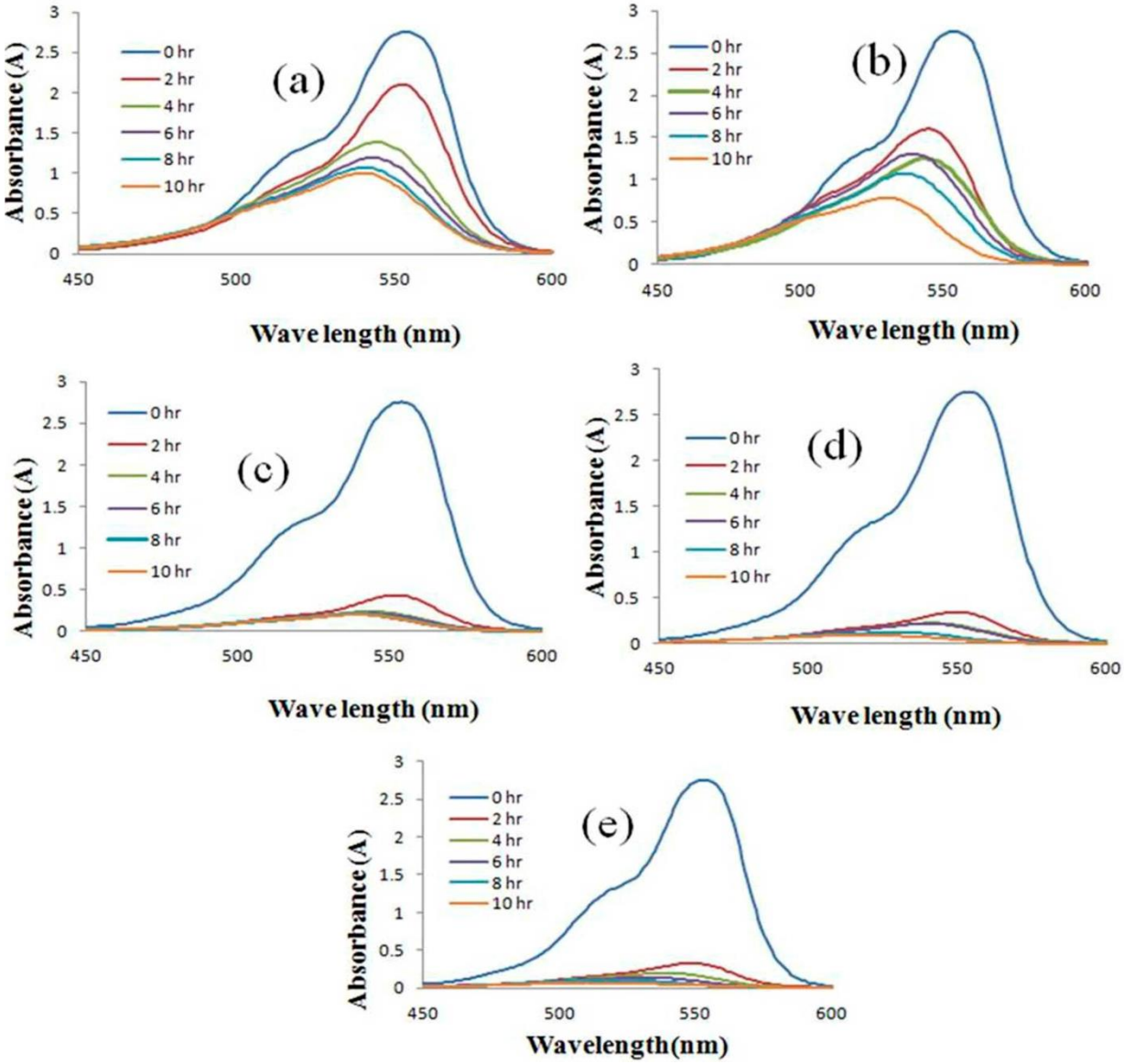

Fig. 6: (a) UV-VIS spectra of rhodamine B dye degraded by (a) pure PCL (b) Fe_2O_3(1 wt%)/PCL nanocomposite, (c) Fe_2O_3(2 wt%)/PCL nanocomposite, (d) Fe_2O_3(4 wt%)/PCL nanocomposite and (e) Fe_2O_3(6 wt%)/PCL nanocomposites.

POM Study

The POM image (Fig. 5) presented that PCL had distinctive crystalline spherulites with Maltese morphology. The maltase type spherulite was also reported by Woo et al. [20]. The spherulites size of PCL is in the range of 15-45 µm and had similar arrangement. Fig 5 b-d showed that spherulites size of PCL was decreased regularly as the amount of Fe_2O_3 nanoparticles were increased in PCL matrix. The decrease in size of spherulites is due to inter molecular interaction between nanoparticle and polymers, which affect the crystallization behavior. The decrease in spherulites size in the case of Fe_2O_3/PCL nanocomposites might be due to nucleation role of Fe_2O_3 nanoparticles on PCL.

Photodegradation study of Rhodamine B

The photodegradation study of rhodamine B was carried out by degrading it under UV-light irradiation in the presence of Fe_2O_3/PCL nanocomposites. Fig 6 a-e shows the UV-VIS spectra of rhodamine B dye before and after UV-irradiation, which is photodegraded by pure PCL and Fe_2O_3/PCL nanocomposites, respectively. The spectra show that

the photodegradation of rhodamine B dye increased as increased the irradiation time and also with increasing the amount of Fe_2O_3 nanoparticles in nanocomposites.

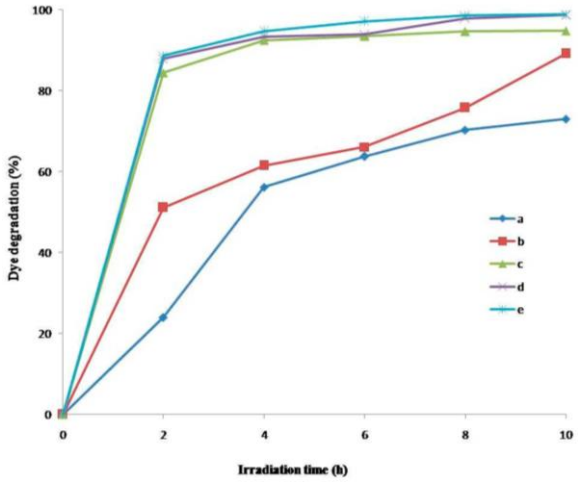

Fig. 7: %degradation comparison of rhodamine as degraded by (a) pure PCL (b) Fe_2O_3(1 wt%)/PCL nanocomposite, (c) Fe_2O_3(2 wt%)/PCL nanocomposite, (d) Fe_2O_3(4 wt%) /PCL nanocomposite, and (e) Fe_2O_3(6 wt%)/PCL nanocomposites.

Conclusion

The morphological study showed that size of Fe_2O_3 nanoparticles were below 250 nm and dispersed well within the PCL matrix. The thermal stability of PCL was improved as increased the quantity of Fe_2O_3 nanoparticles, which mean that the nanoparticles played catalytic role during the thermal degradation of PCL. The DSC analyses show that the Tc of the nanocomposites slightly enhanced as compared to neat PCL because of nucleation role of Fe_2O_3 nanoparticles. The POM analyses showed that the size of Fe_2O_3/PCL nanocomposites spherulites were smaller than neat PCL. The photodegradation study presented that the nanocomposites photodegraded higher quantity of rhodamine B dye as compared to neat PCL.

References

1. V. I. Shadrina, I. A. Bashmakov, V. E. Agabekova and F. N. Kaputskii, Thin Film Net Metal–Polymer Composites, *Russ. J. Gen. Chem.*, **80,** 1064 (2010).
2. M. A. Kudryashov, A. I. Mashin, A. S. Tyurin, G. Chidichimo, G. De Filpo, Metal-Polymer Composite Films Based on Polyacrylonitrile and Silver Nanoparticles. Preparation and Properties, *J. Surf. Invest. X-ray, Synchrotron and Neutron Techn.*, **4,** 437 (2010).
3. Z. Sun, Y. Chen, Q. Ke, Y. Yang, J. Yuan, Photocatalytic Degradation of a Cationic Azo Dye by TiO_2/Bentonite Nanocomposite, *J. Photochem. Photobiol. A Chem.*, **149,** 169 (2002).
4. I. Khan, I. Khan, M. Usman, M. Imran, K. Saeed, Nanoclay-mediated Photocatalytic Activity Enhancement of Copper Oxide Nanoparticles for Enhanced Methyl Orange Photodegradation, *J. Mater. Sci mater-El.*, **31**, 8971 (2020).
5. Y. Chiu, T. M. Chang, C. Chen, M. Sone, Y. Hsu, Mechanistic Insights into Photodegradation of Organic Dyes using Heterostructure Photocatalysts, *Catalysts*, **9**, 430 (2019).
6. I. Khan, M. Sadiq, I. Khan, K. Saeed, Manganese Dioxide Nanoparticles/Activated Carbon Composite as Efficient UV and Visible-Light Photocatalyst. *Environ. Sci. Pollut. Res.*, **26**, 5140 (2019).
7. G. Chen, M. Sun, Q. Wei, Y. Zhang, B. Zhu, B. Du. Ag_3PO_4/Graphene-Oxide Composite with Remarkably Enhanced Visible-Light-Driven Photocatalytic Activity Toward Dyes in Water. *J. Hazard. Mater.*, **244,** 86 (2013).
8. Y. Xia, F. Ma, K. Li, Y. Guo, J. Hu, W. Li, M. Huo, Y. Guo, Mixed Phase Titania Nanocomposite Co-doped with Metallic Silver and Vanadium Oxide: New Efficient Photocatalyst for Dye Degradation, *J. Hazard. Mater.*, **175,** 429 (2010).
9. Ishibashi, Ken-ichi, A. Fujishima, T. Watanabe, K. Hashimoto, Quantum Yields of Active Oxidative Species formed on TiO_2 Photocatalyst, *J. Photochem. Photobiol. A Chem.*, **134,** 139 (2000).
10. E. Volkan, F. Sari, H. Gülce, A. Gülce, A. Avci, Preparation of the New Polyaniline/ZnO Nanocomposite and its Photocatalytic Activity for Degradation of Methylene Blue and Malachite Green Dyes under UV and Natural Sun Lights Irradiations, *Appl. Catal. B Environ.*, **119,** 197 (2012).
11. A. Sadia, M. S. Akhtar, Y. S. Kim, O. -B. Yang, H. -S. Shin, An Effective Nanocomposite of Polyaniline and ZnO: Preparation, Characterizations, and its Photocatalytic Activity, *Colloid Polym. Sci.*, **289,** 415 (2011).
12. R. Saravanan, S. Karthikeyan, V. K. Gupta, G. Sekaran, V. Narayanan, A. Stephen, Enhanced Photocatalytic Activity of ZnO/CuO Nanocomposite for the Degradation of Textile

Dye on Visible Light Illumination, *Mater. Sci. Eng. C.*, **33,** 91 (2013).
13. N. Panda, H. Sahoo, S. Mohapatra, Decolourization of Methyl Orange using Fenton-Like Mesoporous Fe_2O_3–SiO_2 Composite, *J. Hazard. Mater.*, **185,** 359 (2011).
14. S. Ameen, M. S. Akhtar, Y. S. Kim, O. -B. Yang, H. -S. Shin, Synthesis and Characterization of Novel Poly(1-Naphthylamine)/Zinc Oxide Nanocomposites: Application in Catalytic Degradation of Methylene Blue Dye, *Colloid Polym. Sci.*, **288,** 1633 (2010).
15. K. Saeed, S. -Y. Park, H. -J. Lee, J. –B. Baek, W. -S. Huh, Preparation of Electrospun Nanofibers of Carbon Nanotube/Polycaprolactone Nanocomposite, *Polymer*, **47,** 8019 (2006).
16. Z. Shengxiao, X. Zhao, H. Niu, Y. Shi, Y. Cai, G. Jiang, Superparamagnetic Fe_3O_4 Nanoparticles as Catalysts for the Catalytic Oxidation of Phenolic and Aniline Compounds, *J. Hazard. Mater.*, **167,** 560 (2009).
17. K. Saeed, I. Khan, Z. Ahmad, B. Khan, Preparation, Analyses and Application of Cobalt–Manganese Oxides/Nylon 6,6 Nanocomposites, *Polym. Bull.*, **75,** 4657 (2018).
18. K. Saeed, S. –Y. Park, Preparation and Properties of Multiwalled Carbon Nanotube/Polycaprolactone Nanocomposites, *J. Appl. Polym. Sci*., **104,** 1957 (2007).
19. M. T. M. Bizarria, André LF de M. Giraldi, C. M. deCarvalho, J. I. Velasco, M. A. d'Avila, L. H. Mei, Morphology and Thermomechanical Properties of Recycled PET-Organoclay Nanocomposites, *J. Appl. Polym. Sci.*, **104,** 1839 (2007).
20. E. M. Woo, T. K. Mandal, S. C. Lee, Relationships between Ringed Spherulitic Morphology and Miscibility in Blends of Poly(ε-caprolactone) with Poly(benzyl methacrylate) Versus Poly(phenyl methacrylate), *Colloid Polym. Sci.*, **278,** 1032 (2000).